Victor C. Tsai[1]
Seismological Laboratory,
California Institute of Technology,
Pasadena, CA 91125
e-mail: tsai@caltech.edu

James R. Rice
School of Engineering and Applied Sciences,
and Department of Earth
and Planetary Sciences,
Harvard University,
Cambridge, MA 02138
e-mail: rice@seas.harvard.edu

Modeling Turbulent Hydraulic Fracture Near a Free Surface

Motivated by observations of the subglacial drainage of water, we consider a hydraulic fracture problem in which the crack grows parallel to a free surface, subject to fully turbulent fluid flow. Using a hybrid Chebyshev/series-minimization numerical approach, we solve for the pressure profile, crack opening displacement, and crack growth rate for a crack that begins relatively short but eventually becomes long compared with the distance to the free surface. We plot nondimensionalized results for a variety of different times, corresponding with different fracture lengths, and find substantial differences when free-surface effects are important. [DOI: 10.1115/1.4005879]

1 Introduction

Hydraulic fracture has been studied for many years, with numerous studies successfully applying linear elastic fracture mechanics with a variety of flow conditions [1–3]. While near-surface fractures have been studied [4,5], and turbulent flows have been considered [6,7], one variation that seems to have eluded study is that of a fully turbulent near-surface hydraulic fracture. Recent observations in Ref. [8] along with our previous modeling efforts [7] regarding these observations suggest that drainage of supraglacial lakes sometimes results in subglacial flooding that achieves this regime of hydraulic fracture. With this motivation, in this work, we solve a fully turbulent hydraulic fracture problem in which the fracture grows parallel to the free surface and eventually becomes long in comparison to the distance to the free surface. As in our previous work and as in Ref. [9], we use constant pressure inlet conditions, another departure from much of the hydraulic fracture literature [1,3].

2 Model Setup

We consider an impermeable elastic half-space with a crack at depth $z=-H$ (see Fig. 1) parallel to the free surface and of length $2L$ along $-L<x<L$. We assume that this crack, which has rough walls, opens in plane strain subject to a constant pressure input p_I at its center that drives a strongly turbulent fluid flow into the crack and causes it to grow (p_I corresponds to inlet pressure minus initial compressive stress $\sigma_0=-\sigma_{zz}$ from overburden). To model this hydraulic fracture close to a free surface, we follow the approach of Ref. [7] in which a Manning-Strickler model [10–12] for fully turbulent flow resistance is used along with standard elasticity [13,14] and fluid mechanics to solve for the pressure distribution $p(x,t)$, opening displacement $w(x,t)$, thickness-averaged fluid velocity $U(x,t)$ within the crack, and crack growth rate $U_{tip}(t)=dL(t)/dt$. The primary difference between Ref. [7] and the present work is that the fracture is no longer assumed to be far from the free surface. Due to the need of now accounting for the free surface, the elasticity equations are modified from what was previously used. Instead, we follow the formulation of Refs. [15,16] for the elasticity relationships.

2.1 Governing Equations.

As in Ref. [7], when the Reynolds number Re is sufficiently large, flow resistance is determined only by wall roughness, and the rough-wall turbulent flow resistance can be approximated by a Manning-Strickler model [12] in which the Darcy-Weisbach friction factor $f=f_0(k/w)^{1/3}$. Here f is defined so that the average of drag stresses on the upper and lower channel walls is $f\rho U^2/8$, $f_0\approx 0.143$ [7,17,18], k is the Nikuradse wall roughness height [17,18], and w is the opening thickness of the channel. f is well characterized for pipe flow [17,18] and has been generalized to our slit-like channel using the concept of hydraulic radius [12,17]. This turbulent flow model then provides one relationship between $p(x,t)$, $w(x,t)$, and $U(x,t)$ as

$$-\frac{\partial p}{\partial x}=\frac{f_0\rho U^2}{4}\frac{k^{1/3}}{w^{4/3}} \tag{1}$$

for $x>0$ (and negative of this for $x<0$). Conservation of mass for an incompressible fluid provides a second relationship as

$$\frac{\partial(wU)}{\partial x}+\frac{\partial w}{\partial t}=0 \tag{2}$$

The elastic governing equations are assumed to be those of quasistatic plane strain elasticity, which is found to be a good approximation since crack tip speeds $U_{tip}=dL/dt$ are found to be a very small fraction of elastic wave speeds for this class of hydraulic fracture problems [1,3,19]. In order to account for free-surface effects, we use the formulation of Erdogan et al. [15], which implies that

$$0=-\sigma_{xz}=\int_{-L}^{L}\left[\left(\frac{1}{s-x}+k_{11}\right)\frac{\partial u}{\partial s}+k_{12}\frac{\partial w}{\partial s}\right]ds \tag{3a}$$

and

$$-\frac{4\pi p(x)}{E'}=\int_{-L}^{L}\left[k_{21}\frac{\partial u}{\partial s}+\left(\frac{1}{s-x}+k_{22}\right)\frac{\partial w}{\partial s}\right]ds \tag{3b}$$

where $u=u(s,t)$, $w=w(s,t)$, and the $k_{ij}=k_{ij}(x,s;H)$ are elasticity kernels given in Ref. [15], with notable typographical error that Eq. (7.93) of Erdogan et al. should read "$k_{12}=-k_{21}=\ldots$" instead of "$k_{12}=k_{21}=\ldots$". Correction of this typo has been discussed explicitly in Ref. [20] and explains the differences between the results shown in Refs. [15,16]. As in Refs. [3,7], Eq. (3*a*) assumes that the shear stress is zero, consistent with the expectation that shear stresses on the crack walls are small compared to fluid pressures. This expectation can be verified by observing that for the geologic applications in mind, $P_I\ll E'$, which implies that $w_0/L\ll 1$, which in turn implies that lubrication theory approximately applies (i.e., wall shear stress τ_{wall} satisfies $2\tau_{wall}=-w\cdot dp/dx\sim p_I\cdot w_0/L\ll p_I$).

The final governing equation is the fracture criterion,

[1]Corresponding author.

Contributed by the Applied Mechanics Division of ASME for publication in the Journal of Applied Mechanics. Manuscript received September 19, 2011; final manuscript received January 11, 2012; accepted manuscript posted February 6, 2012; published online April 4, 2012. Assoc. Editor: Nadia Lapusta.

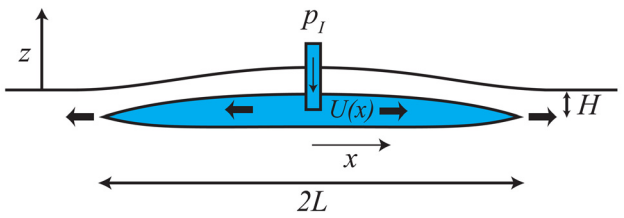

Fig. 1 Schematic for turbulent hydraulic fracture

$$K_I = K_{Ic} = 0 \tag{4}$$

where K_I is the mode I stress intensity factor, K_{Ic} is the fracture toughness, and K_{Ic} is assumed to be small enough compared to a nominal K_I (say, $p_I\sqrt{\pi L}$) associated with the loading that we may approximate it as zero. As discussed in Refs. [2,3,7], this assumption is appropriate as long as L is relatively long. We note that for the motivating problem of a draining meltwater lake, the constant p_I condition (as assumed) is appropriate and that for this condition, the $K_{Ic} = 0$ assumption becomes progressively better as the crack grows longer [7]. We further note that the K_{Ic} along a glacier-bedrock interface is likely to be less than the K_{Ic} within pure ice, thus, encouraging growth parallel to the free surface, as assumed.

The boundary conditions that close the system of equations given by Eqs. (1)–(4) can be expressed as $p(0,t) = p_I$, $w(L,t) = 0$, $U(L,t) = U_{tip} = dL/dt$ [7].

2.2 Solution Method. At a given time step, we solve the governing equations by the following hybrid Chebyshev/series-minimization method. First, we nondimensionalize x, p, u, w, U, and t as $\hat{x} = x/L$, $\hat{p} = p(x,t)/p_I$, $\hat{u} = uE'/(p_I L)$, $\hat{w} = wE'/(p_I L)$, $\hat{U} = U/U_{tip}$, and $\hat{t} = tU_{tip}/L$, where

$$U_{tip} = \phi U_S \equiv \phi\sqrt{\frac{p_I}{\rho}}\left(\frac{p_I}{E'}\right)^{2/3}\left(\frac{L}{k}\right)^{1/6} \tag{5}$$

Next, we take $\hat{p}(\hat{x},\, t)$ and $\hat{w}(\hat{x},\, t)$ to be given by

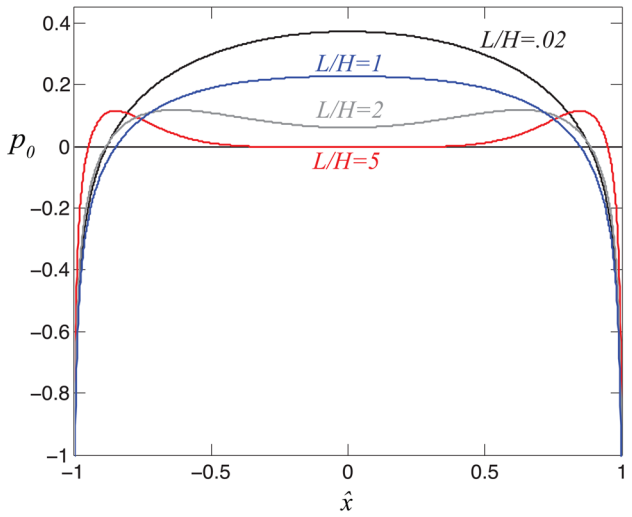

Fig. 2 Leading order pressure term p_0 corresponding with $a_0 w_0 = a_0[(1-\hat{x})/2]^{6/7}$ for different values of L/H (0.02 = black, 1 = blue, 2 = gray, and 5 = red). (Colors may be viewed in the online version of the paper.)

$$\frac{\hat{p}(\hat{x},\, t)}{D} = \sum_{k=0}^{2N} a_k p_k(\hat{x}) = a_0 p_0(\hat{x}) + \sum_{k=1}^{N} a_{2k-1}\left[c_{2k-1} - |\hat{x}|^{2k-1}\right] + \sum_{k=1}^{N} a_{2k}\left[c_{2k} - U_{2k}(\hat{x})\right] \tag{6}$$

and

$$\frac{\hat{w}(\hat{x},\, t)}{D} = \sum_{k=0}^{2N} a_k w_k(\hat{x}) = a_0\left(\frac{1-\hat{x}}{2}\right)^{6/7} + \sum_{k=1}^{2N} a_k w_k(\hat{x}) \tag{7}$$

where $U_k(x)$ are Chebyshev polynomials of the second kind, a_k, c_k, and D are coefficients to be determined, and p_k and w_k are chosen to satisfy Eq. (3). This term-wise satisfaction of Eq. (3) is done by the Chebyshev method of Ref. [15], with p_k and w_k being

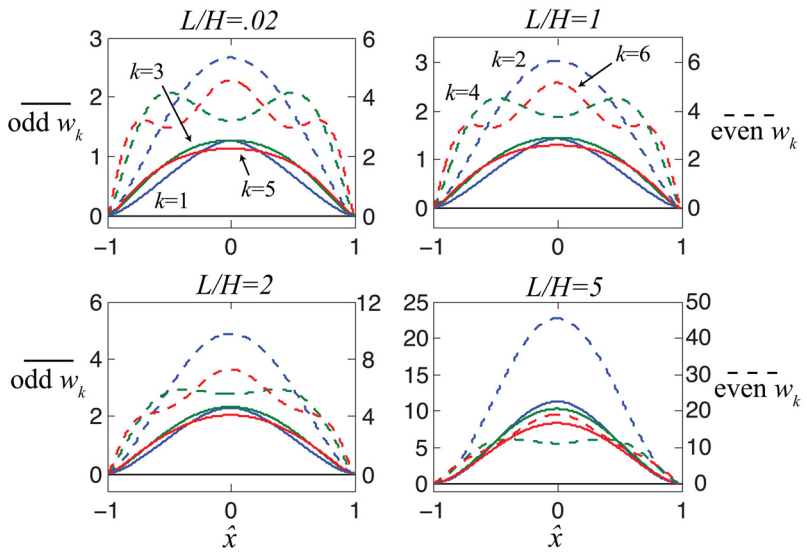

Fig. 3 Crack openings w_k, from $k = 1$ to 6, for different values of L/H. Odd w_k are in solid lines and units are on the left axis. Even w_k are in dashed lines and units are on the right axis. Blue, green and red colors correspond to 1,3,5 for odd and 2,4,6 for even, respectively. (Color may be viewed in the online line version of the paper.)

expressed as a Chebyshev series whose coefficients can be solved algebraically once certain integrals are computed numerically by Chebyshev-Gauss quadrature. The term w_0 is chosen to asymptotically solve the governing equations as in Ref. [7], and the coefficients c_k are chosen such that each term of the series satisfies Eq. (4). The p_0 and w_k for a few choices of L are plotted in Figs. 2 and 3. It may be noted that since p_k and w_k pairwise satisfy the elastic governing equations, then by linearity $\hat{p}$ and $\hat{w}$ also satisfy the elastic equations, but they do not yet satisfy the fluid equations or boundary conditions.

Choosing $a_0 \equiv 14\tan(\pi/7)/3$ as in Ref. [7], then asymptotic analysis shows that

$$\hat{p} \to -D[(1-\hat{x}^2)/2]^{-1/7} \text{as } \hat{x}^2 \to 1 \tag{8}$$

As in Ref. [7], this singular solution neglects fluid lag effects [21]. Taking the same limit ($\hat{x} \to 1$) in Eq. (1) then yields

$$\phi = \frac{2a_0^{2/3}D^{7/6}}{(7f_0)^{1/2}} \tag{9}$$

and Eq. (1) with Eq. (2) can be rewritten as

$$\frac{-\left(\sum_k a_k w_k\right)^{10/3}}{a_0^{4/3}/7}\frac{\partial\left[\sum_k a_k p_k\right]}{\partial \hat{x}} = \left[\int_{\hat{x}}^{1}\frac{\partial\left(\sum_k a_k w_k\right)}{\partial \hat{t}}d\hat{s}\right]^2 \tag{10}$$

We then approximately solve Eq. (10) by choosing a_k to minimize the normalized error (over equally spaced points from $\hat{x}=0$ to $\hat{x}=1$) between the right-hand-side (RHS) and left-hand-side (LHS) under the constraint that w is always positive. In order to evaluate the RHS of Eq. (10), a backwards Euler method is used to approximate $\partial w/\partial t$, using the known $w(x,t_{-1})$ and the unknown $w(x,t_0)$ to compute an approximate $\partial w/\partial t \approx [w(x,t_0)-w(x,t_{-1})]/\Delta t$. In the first time step, the self-similar solution of Ref. [7] is used to estimate $\partial w/\partial t$ instead of the backwards Euler method.

2.3 Solution. Using the solution method described in Sec. 2.2, we solve for the growth of the crack starting from an initial crack length that is small compared with the distance to the free surface ($L/H = 0.02 \ll 1$) up to $L/H = 5$. As in Refs. [3,7], we find that taking a small number of terms in Eqs. (6) and (7) adequately represents the solution. In particular, we use terms up to $k=6$, corresponding to choosing $N=3$. As discussed earlier, we initialize conditions to be equal to the self-similar solution of Ref. [7], with the modification that we now use six terms ($N=3$) instead of four terms ($N=2$) to approximate the self-similar solution as well. We take time steps that correspond to $\Delta L/L = 0.05$.

Snapshots of the scaled pressure distribution $\hat{p}(\hat{x})$ and scaled crack opening displacement $\hat{w}(\hat{x})$ are shown in Figs. 4 and 5, respectively, for different times that correspond to the marked L/H. Also, the average opening $\hat{w}_{avg}$ along the crack (note that $2w_{avg}L$ is the volume per unit thickness of fluid within the opened fracture) and the scaled crack tip velocity $\phi = U_{tip}/U_S$ are given in Figs. 6 and 7, respectively, as functions of L/H. The pressure distribution and crack opening at $L/H = 0.02$ are virtually identical to those of the self-similar quantities of Ref. [7] (for $L/H \ll 1$). As L/H grows, the pressure falls more rapidly as one moves from the inlet ($\hat{x}=0$) to the crack tip ($\hat{x}=1$) (see Fig. 4). For drainage of surface water at hydrostatic pressure under an ice sheet, we observe that $p_I/\sigma_0 \approx 0.1$ so that atmospheric pressure is not reached until $\hat{p} \approx -10$.

As expected, the crack opening increases rapidly with increasing L/H such that the opening for $L/H = 5$ is about 20 times

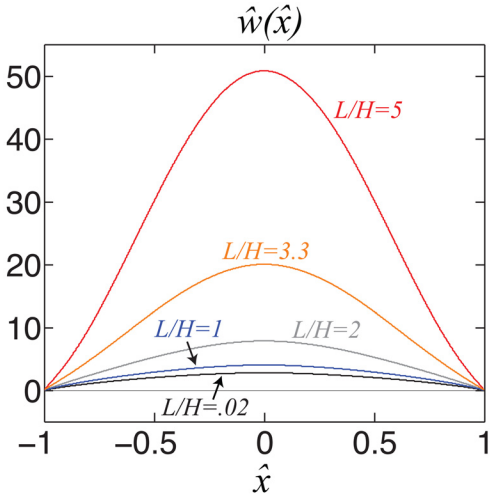

Fig. 5 Scaled opening $\hat{w}(\hat{x})$ plotted for different values of L/H (colors as in Fig. 4, with additional orange curve at $L/H = 3.3$). (Colors may be viewed in the online version of the paper.)

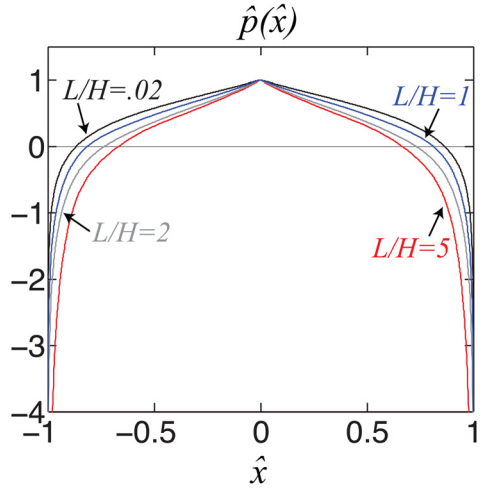

Fig. 4 Scaled pressure $\hat{p}(\hat{x})$ plotted for different values of L/H (colors are as in Fig. 2). (Colors may be viewed in the online version of the paper.)

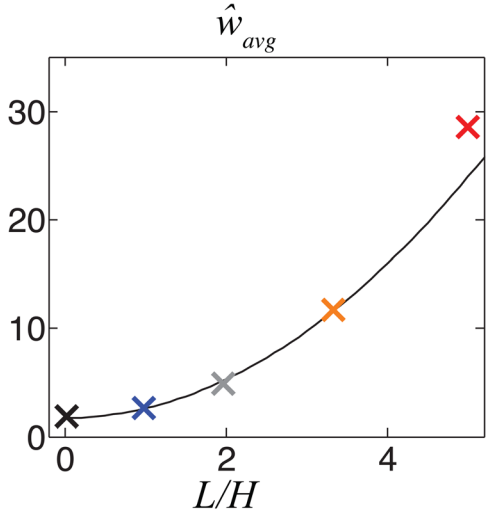

Fig. 6 Scaled average opening $\hat{w}_{avg}$ versus L/H (colors as in Fig. 5). Solid line is the polynomial fit discussed in the text. (Colors may be viewed in the online version of the paper.)

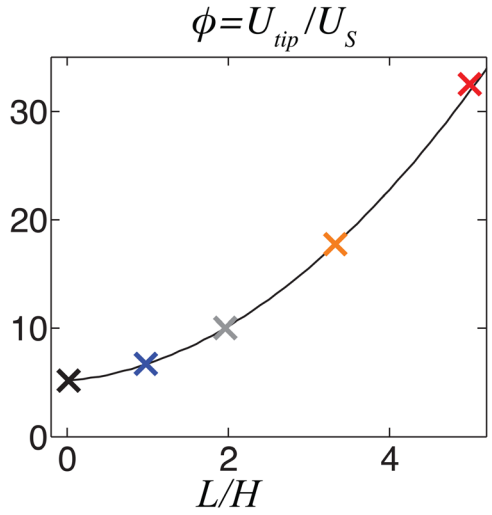

Fig. 7 Scaled crack-tip velocity $\phi \equiv U_{tip}/U_S$ versus L/H (colors as in Fig. 5). Solid line is the polynomial fit discussed in the text. (Colors may be viewed in the online version of the paper.)

larger than the opening for $L/H = 0.02$ (see Fig. 6) and, therefore, much larger than in the $L \ll H$ solution of Ref. [7]. To quantify this growth, we observe that the average opening grows close to quadratically with L/H and that the data up to $L/H = 3.3$ are fit reasonably well with $\hat{w}_{avg} \approx 1.72 + 0.89(L/H)^2$. This fit is accurate to within $\approx 5\%$ for $L/H \leq 3.3$ but has substantial error for $L/H > 3.3$ (at $L/H = 5$, the fit is 16% off).

Finally, the crack-tip velocity (see Fig. 7) also grows substantially, with a normalized speed that is six to seven times that of the original normalized speed (this is an increase on top of the slow $L^{1/6}$ growth inherent in the scaling of U_S; see Eq. (5)). Performing a 2nd-degree polynomial fit to the data up to $L/H = 3.3$ yields a reasonable fit as $\phi \approx 5.13 + 0.64(L/H) + 0.94(L/H)^2$. This fit is accurate to within 5% for the entire range of the plot (up to $L/H = 5$). Given $\hat{w}_{avg}$ and ϕ, we can then calculate a 2D total inflow rate Q as

$$\begin{aligned} Q &= \frac{d(2w_{avg}L)}{dt} = \frac{2p_I}{E'}\frac{d(\hat{w}_{avg}L^2)}{dt} \\ &= \frac{2p_I}{E'}\frac{\partial(\hat{w}_{avg}(L/H)L^2)}{\partial L}\frac{dL}{dt} \\ &= \frac{2p_I U_S}{E'}\frac{\partial(\hat{w}_{avg}(L/H)L^2)}{\partial L}\phi \end{aligned} \tag{11}$$

Here, based on the polynomial fit above for $\hat{w}_{avg}$, $\partial(\hat{w}_{avg}(L/H)L^2)/\partial L \approx 2L(1.72 + 1.78L^2/H^2)$.

Thus, normalizing Q as $\hat{Q} = QE'/(4 \cdot 1.72 \cdot 5.13 p_I L U_S)$, where the terms with decimal points correspond respectively to $\hat{w}_{avg}$ and ϕ when $L/H \to 0$, we have $\hat{Q} \approx 1$ when $L \ll H$, but $\hat{Q} \approx 2.7$ when $L = H$, $\hat{Q} \approx 10$ when $L = 2H$, and $\hat{Q} \approx 31$ when $L = 3H$. While these indicate very substantial increases of Q with L for the conditions analyzed, of fixed inlet pressure p_I, it is important to recognize that for a given L, Q is proportional to $p_I U_S$, and hence to $p_I^{13/6}$. Thus, in an application like for rapid draining of a supraglacial lake along a crevasse/moulin system through an ice sheet [8], driving a hydraulic fracture (i.e., a region of flotation) along its bed, resistance to the vertical flow would increase with increasing flow rate, and hence decrease p_I [7]. For example, decrease of p_I to $0.50p_I$ would decrease Q to $0.22Q$ in the solution presented (which is for the case that p_I remains constant as the fracture grows).

3 Discussion and Conclusions

This work presents numerical solutions to a turbulent hydraulic fracture close to a free surface. It is a natural extension of a large literature of hydraulic fracture problems [1–3,6,7]. Unlike previous work, we solve the problem for the case in which the fracture grows into the range where it becomes close to the free surface, the fluid flow is in the fully turbulent flow regime (approximated by a Manning-Strickler model), and the input pressure remains constant. The problem, therefore, represents a different physical set of constraints compared with previous studies.

As briefly mentioned in the Introduction, previous work suggests that the current model is applicable to at least one important class of problems, that of drainage of supraglacial lakes into subglacial lakes, as observed in Ref. [8]. However, before the current modeling can be successfully applied to this class of problems, our previous work [7] has shown that it is important to correctly account for the vertical drainage of water, a task that remains to be done in a completely self-consistent manner. The strong sensitivity of the present work on L/H underscores the necessity to understand this vertical drainage better before such solutions can be applied with confidence. Despite this known difficulty, the solution that we have constructed represents a necessary first step in the path towards understanding such problems. For example, our solution has more realistic pressure boundary conditions compared with other models of similar processes [22,23], which do not attempt to satisfy these boundary conditions.

The solutions are shown to deviate significantly from the self-similar solution in a homogeneous whole-space once $L/H \ll 1$ is no longer satisfied. In particular, the pressure distribution is moderately affected, the crack opening and total inflow rate are substantially larger, and the crack growth rate is also significantly larger than when $L/H \ll 1$. These results provide important quantitative constraints on how turbulent hydraulic fracture is different as free-surface effects become significant.

Acknowledgment

This research was supported by National Science Foundation OPP Grant No. ANT-0739444 to Harvard University and a Mendenhall Postdoctoral Fellowship of the United States Geological Survey to VCT.

Nomenclature

D = coefficient in series for p and w
E = Young's modulus
E' = $E/(1 - \nu^2)$ = effective modulus in plane strain
H = distance of crack from free surface
K_I = mode I stress intensity factor
K_{Ic} = mode I fracture toughness
L = half length of crack
Q = two dimensional total fluid flow rate
$U(x,t)$ = average fluid speed within crack
U_{tip} = crack tip speed
U_S = velocity scale
U_k = Chebyshev polynomials of the second kind
a_k = coefficients in series for p and w
f = Darcy-Weisbach friction factor
k = Nikuradse roughness height
k_{ij} = Erdogan elasticity kernels
$p(x,t)$ = pressure distribution along crack
p_I = constant input pressure at center of crack
p_0 = leading-order pressure term corresponding with w_0
p_k = terms in pressure series corresponding with w_k
t = time
$u(x,t)$ = crack shear displacement
$w(x,t)$ = crack opening displacement
w_{avg} = average crack opening displacement
w_k = terms in crack opening series corresponding with p_k
x = horizontal position along crack
z = vertical position
ϕ = constant for velocity scale
ρ = fluid density

σ_{ij} = stress components
τ_{wall} = wall shear stress
$\hat{\cdot}$ = nondimensionalized

References

[1] Spence, D. A., and Sharp, P., 1985, "Self-Similar Solutions for Elastohydrodynamic Cavity Flow," Proc. R. Soc. London, Ser. A, **400**, pp. 289–313.
[2] Desroches, J., Detournay, E., Lenoach, B., Papanastasiou, P., Pearson, J. R. A., Thiercelin, M., and Cheng, A., 1994, "The Crack Tip Region in Hydraulic Fracturing," Proc. R. Soc. London, Ser. A, **447**, pp. 39–48.
[3] Adachi, J. I., and Detournay, E., 2002, "Self-Similar Solution of a Plane-Strain Fracture Driven by a Power-Law Fluid," Int. J. Numer. Analyt. Meth. Geomech., **26**, pp. 579–604.
[4] Zhang, X., Detournay, E., and Jeffrey, R., 2002, "Propagation of a Penny-Shaped Hydraulic Fracture Parallel to the Free-Surface of an Elastic Half-Space," Int. J. Fract., **115**, pp. 125–158.
[5] Bunger, A. P., and Detournay, E., 2005, "Propagation of a Penny-Shaped Fluid-Driven Fracture in an Impermeable Rock: Asymptotic Solutions," Int. J. Solids Struct., **39**, pp. 6311–6337.
[6] Nilson, R. H., 1981, "Gas-Driven Fracture Propagation," J. Appl. Mech., **48**, pp. 757–762.
[7] Tsai, V. C., and Rice, J. R., 2010, "A Model for Turbulent Hydraulic Fracture and Application to Crack Propagation at Glacier Beds," J. Geophys. Res., **115**, pp. 1–18.
[8] Das, S., Joughin, I., Behn, M. D., Howat, I. M., King, M. A., Lizarralde, D., and Bhatia, M. P., 2008, "Fracture Propagation to the Base of the Greenland Ice Sheet During Supraglacial Lake Drainage," Science, **320**, pp. 778–781.
[9] Rubin, A. M., 1993, "Dikes vs. Diapirs in Viscoelastic Rock," Earth Planet. Sci. Lett., **119**, pp. 641–659.
[10] Manning, R., 1891, "On the Flow of Water in Open Channels and Pipes," Trans. Inst. Civil Eng., **20**, pp. 161–207.
[11] Strickler, A., 1923, "Beitrage zur frage der geschwindigkeitsformel und der rauhigkeitszahlen fur strome, kanale und geschlossene leitungen," Technical report, Mitteilungen des Eidgenossischen Amtes fur Wasserwirtschaft 16, Bern, Switzerland.
[12] Strickler, A., 1981, *Contributions to the Question of a Velocity Formula and Roughness Data for Streams, Channels and Closed Pipelines*, T. Roesgen and W. R. Brownlie, translators, W. M. Keck Lab of Hydraulics and Water Resourses, California Institute of Technology, Pasadena, CA.
[13] Timoshenko, S. P., and Goodier, J. N., 1987, *Theory of Elasticity*, 3rd ed., McGraw-Hill, New York.
[14] Muskhelishvili, N. I., 1953, *Some Basic Problems of the Mathematical Theory of Elasticity*, 3rd ed., Noordhoff Ltd., Groningen, Holland.
[15] Erdogan, F., Gupta, G. D., and Cook, T. S., 1973, "Numerical Solution of Singular Integral Equations," *Methods of Analysis and Solution of Crack Problems. Recent Developments in Fracture Mechanics*, G. C. Sih, ed., Leyden, Noordhoff Int. Pub., San Diego, CA, pp. 368–425.
[16] Higashida, Y., and Kamada, K., 1982, "Stress Fields Around a Crack Lying Parallel to a Free Surface," Int. J. Fract., **19**, pp. 39–52.
[17] Rubin, H., and Atkinson, J., 2001, *Environmental Fluid Mechanics*, Marcel Dekker, Inc., New York.
[18] Gioia, G., and Chakraborty, P., 2006, "Turbulent Friction in Rough Pipes and the Energy Spectrum of the Phenomenological Theory," Phys. Rev. Lett., **96**, pp. 1–4.
[19] Lister, J. R., 1990, "Buoyancy-Driven Fluid Fracture: The Effects of Material Toughness and of Low-Viscosity Precursors," J. Fluid Mech., **210**, pp. 263–280.
[20] Viesca, R. C., and Rice, J. R., 2011, "Elastic Reciprocity and Symmetry Constraints on the Stress Field due to a Surface-Parallel Distribution of Dislocations," J. Mech. Phys. Solids, **59**, pp. 753–757.
[21] Garagash, D. I., and Detournay, E., 2005, "Plane-Strain Propagation of a Fluid-Driven Fracture: Small Toughness Solution," J. Appl. Mech., **72**, pp. 916–928.
[22] Schoof, C., 2010, "Ice-Sheet Acceleration Driven by Melt Supply Variability," Nature, **468**, pp. 803–806.
[23] Pimentel, S., and Flowers, G. E., 2011, "A Numerical Study of Hydrologically Driven Glacier Dynamics and Subglacial Flooding," Proc. R. Soc., Math. Physic. Eng. Sci., **467**, pp. 537–558.